EM Analysis of Vane-Loaded RF Interaction Structure for its Potential Application in Gyrotrons

R. K. Singh* and Chahat Jain**
*Dept. of Electronics Engg., Guru Nanak Dev Engg. College, Ludhiana, India - 141001
Email: rajivinbhu@gmail.com
**Dept. of Electronics Engg., Guru Nanak Dev Engg. College, Ludhiana, India - 141001
Email: chahatjain26@gmail.com

Abstract: All-metal RF interaction structures have potential to be used in high-power high-frequency gyro-devices. With this intension, the vane-loaded all-metal RF interaction structure has been field analyzed in this paper. Electromagnetic fields in various regions of the structure, boundary conditions, and finally dispersion relation for the structure have been derived starting from the basic principles. Dispersion relation has been solved using Powel-Dogleg method. Validation of the present analysis has been done for the special case of zero vane angle, and vane depth equal to outer radius of structure wall radius, which is identified as the dispersion relation of the TE_{0n} mode of a smooth wall cylindrical waveguide, that is, of an unloaded waveguide. Parametric analysis on dispersion characteristic revealed that numbers of vanes and angular width of the vanes are more sensitive than the radial depth of the vanes. It has been found that dispersion shaping using vane-loaded structure results in mode-rarefaction which may be advantageous for avoiding mode-competition in over-moded operation of gyro-devices.

Keywords: Vane-loaded RF structure, Gyrotron, Field-matching technique, Dispersion, Azimuthally symmetric modes.

Introduction

The developments of the gyrotrons, the gyro-klystrons and the gyro-TWTs (travelling wave tube) have received the maximum attention in the development of gyro-device. The gyrotrons find application as high-power millimeter wave sources, for instance, in plasma heating for controlled thermonuclear reactor and in material processing. Out of the gyro-klystron and the gyro-TWT, the former that employs resonant interaction cavities, as in the conventional slow-wave klystron, has a lesser bandwidth than the latter that uses a non-resonant waveguide interaction structure. Therefore, the gyro-klystron amplifiers, though they have potential applications in linear accelerators, are not preferred to the gyro-TWTs, which have a wider bandwidth potential, for application in high information density communication systems and high-resolution radars in the high power, millimeter-wave frequency regime [1].

It is obvious that, in order to achieve wideband performance of a gyro-TWT, one has to realise the grazing intersection between the beam-mode and waveguide-mode $\omega-\beta$ dispersion characteristics over a wide range of frequencies. One of the methods of broadbanding a gyro-TWT is to taper the cross section of the waveguide and synchronously profile the magnetic flux density. This method gives wide bandwidths but at the cost of the gain of the device [2]. This is because different smaller length portions of the interaction length of different cross sections become effective for different operating frequency ranges over the amplification band of the device. Alternatively, one may load the wall of a non-tapered waveguide either by dielectric lining its wall or by placing a dielectric rod at the axis of the guide to straighten the waveguide-mode dispersion characteristics over a wider frequency range for wideband grazing intersection with the beam-mode dispersion characteristics, which is essentially a straight line [3]. Consequently, this results in a wideband gain-frequency response of the device. In another method of broadbanding a gyro-TWT, a two-section dielectric loading was suggested [4]. However, the method of dielectric loading the waveguide for broadbanding a gyro-TWT entails the risk of dielectric charging and heating the dielectric if is lossy, a problem that has to be alleviated by the application of a thin metal coating on the dielectric, as mentioned earlier with reference to the dielectric-lined waveguide wall for an SWCA (slow wave cyclotron amplifier) [5]. This calls for an all-metal loading of the waveguide for shaping of the dispersion characteristics with a view to broadbanding a gyro-TWT [6]. One such all-metal structure is a helical waveguide that contains a circular waveguide with helically grooved wall [2]. The structure shows the potential for resulting in a nearly straight-line waveguide-mode dispersion characteristic that can be made coalescent with the beam-mode dispersion line for a wide range of frequencies, near the zero axial phase propagation constant β thereby corresponding to a small Doppler shift βv_z (v_z being axial velocity of the beam). Thus, while broadbanding the gyro-TWT, the method allows a significant reduction in the sensitivity of the device to the beam velocity spread [7]. Theoretical investigations were also made into the problem of shaping the structure dispersion

characteristics by a helix placed close to the waveguide wall with a view to achieving the desired wideband coalescence for wideband performance of a gyro-TWT [3]. Finally, two types of interaction structures, a circular waveguide loaded with axially periodic annular metal discs, which has been studied in the slow-wave regime for a conventional TWT for high gains [8], though not for wide bandwidths, and which is more well known for its application in the linear accelerator; and a cylindrical waveguide, provided with wedge-shaped metal vanes projecting radially inward from the wall of the guide (vane-loaded RF interaction structure), have shown potential as a fast-wave structure for wideband gyro-TWTs, with its dispersion characteristics controllable by the adjustment of the structure parameters. However, the vane loading of cylindrical waveguide was also suggested for gyro-TWTs but with a different purpose – to meet the challenge of building up gyrotrons with low energy beam and low magnetic field with good mode selectivity and high efficiency [9].
In this paper, an electromagnetic analysis of vane-loaded RF interaction structure has been developed, starting from basic principles, to study the effect of vane parameters variations on the dispersion characteristics of the gyrotron device. Results have been thoroughly discussed and conclusions have been drawn mentioning the future aspects of the analysis.

The Vane-Loaded RF Interaction Structure

The present analysis considers a cylindrical waveguide, provided with wedge-shaped metal vanes projecting radially inward from the wall of the guide (Fig. 1).

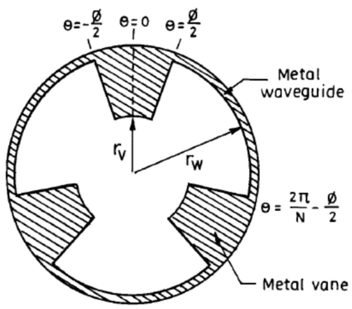

Figure 1. Cross-sectional view of vane-loaded RF interaction structure

For the analysis, two regions in the structure have been identified: (i) the free-space circular-cylindrical region, radially extended between the axis of the guide and the beginning of the vane tips (region 1); and (ii) the free-space wedge-shaped sectorial region between the vanes, radially extending from the beginning of the vane tips up to the inner wall of the waveguide (region 2) (Fig. 1).

EM Field Analysis

Keeping in mind the potential application of the structure in wide-band gyro-TWTs, one would be interested only in the TE-mode interaction, which maximizes at or near the grazing point intersection of the waveguide-mode dispersion hyperbola with the beam-mode dispersion line, where the interaction in the transverse magnetic (TM) mode becomes negligible.
For the structure under consideration, the electromagnetic (EM) field expressions may be written in the cylindrical system of coordinates (r,θ,z), incorporating the angular dependence that takes into account the angular periodicity of the vanes. The angular periodicity of the vanes gives rise to angular harmonics. Owing to the presence of these angular harmonics, the RF quantities will vary with θ as $\exp(jm(2\pi/\phi)\theta)=\exp(jmN\theta)$, where $\phi(=2\pi/N)$ is the angular periodicity of the vanes, N is the number of vanes, and m is an integer representing the angular harmonics. In addition, we consider the time and the axial dependence of the RF quantities as $\exp(j(\omega t-\beta z))$, ω and β being the angular frequency and the axial phase propagation constant, respectively. In view of the above RF dependence, the wave equation in the axial component of the magnetic field intensity H_z, for the waveguide excited in the TE mode, may be written as [1]

$$\left(\frac{\partial^2}{\partial r^2}+\frac{1}{r}\frac{\partial}{\partial r}+k_t^2-\frac{(mN)^2}{r^2}\right)H_z=0 \tag{1}$$

where, $k_t=\left(k_o^2-\beta^2\right)^{1/2}$ is the transverse propagation constant, which is a real quantity for $k_o>\beta$, corresponding to a fast wave-mode. $k_o=\omega/c$ and β are the free-space propagation constants and the axial phase propagation constants, respectively. k_t is defined as the cutoff wave number $k_c(=\omega_{cut}/c)$, which is the value of k_o corresponding to $\beta=0$, where ω_{cut} is the cutoff frequency of the waveguide, and k_c the cutoff wavenumber.

The solution of equation (1) in the two regions of the structure (Fig. 1) is:

$$H_{z,p} = \sum_{m=-\infty}^{\infty} \left(A_{m,p} J_{mN} \{k_c r\} + B_{m,p} Y_{mN} \{k_c r\} \right) \tag{2}$$

where $A_{m.p}$ and $B_{m,p}$ are the field constants. $p=1$ refers to the region 1 $(0 \le r \le r_V \,; 0 \le \theta \le 2\pi)$, and $p=2$ to region 2 $(r_V \le r \le r_W \,; \varphi/2 \le \theta \le 2\pi/N - \varphi/2)$, where r_V is the inner radius of the vane edge and r_W is the inner radius of the waveguide wall. J_{mN} and Y_{mN} are the $(mN)^{th}$ order ordinary Bessel functions of the first and second kinds, respectively. The remaining relevant field expressions can be derived, for the TE mode, with the help of equation (2) and using Maxwell's equations [1].

The field equations in the region 1 can be written as:

$$E_{z,1} = 0 \tag{3}$$

$$H_{z,1} = \sum_{m=-\infty}^{\infty} \left(A_{m,1} J_{mN} \{k_c r\} + B_{m,1} Y_{mN} \{k_c r\} \right) \tag{4}$$

$$E_{r,1} = \sum_{m=-\infty}^{\infty} -\left(mN\omega\mu_o / \left(k_c^2 r\right)\right)\left(A_{m,1} J_{mN} \{k_c r\} + B_{m,1} Y_{mN} \{k_c r\} \right) \tag{5}$$

$$H_{r,1} = \sum_{m=-\infty}^{\infty} -\left(j\beta / (k_c)\right)\left(A_{m,1} J'_{mN} \{k_c r\} + B_{m,1} Y'_{mN} \{k_c r\} \right) \tag{6}$$

$$E_{\theta,1} = \sum_{m=-\infty}^{\infty} -\left(j\omega\mu_o / (k_c)\right)\left(A_{m,1} J'_{mN} \{k_c r\} + B_{m,1} Y'_{mN} \{k_c r\} \right) \tag{7}$$

$$H_{\theta,1} = \sum_{m=-\infty}^{\infty} -\left(mN\beta / \left(k_c^2 r\right)\right)\left(A_{m,1} J_{mN} \{k_c r\} + B_{m,1} Y_{mN} \{k_c r\} \right) \tag{8}$$

Similarly, the field equations in the region 2 can be written as:

$$E_{z,2} = 0 \tag{9}$$

$$H_{z,2} = \sum_{m=-\infty}^{\infty} \left(A_{m,2} J_{mN} \{k_c r\} + B_{m,2} Y_{mN} \{k_c r\} \right) \tag{10}$$

$$E_{r,2} = \sum_{m=-\infty}^{\infty} -\left(mN\omega\mu_o / \left(k_c^2 r\right)\right)\left(A_{m,2} J_{mN} \{k_c r\} + B_{m,2} Y_{mN} \{k_c r\} \right) \tag{11}$$

$$H_{r,2} = \sum_{m=-\infty}^{\infty} -\left(j\beta / (k_c)\right)\left(A_{m,2} J'_{mN} \{k_c r\} + B_{m,2} Y'_{mN} \{k_c r\} \right) \tag{12}$$

$$E_{\theta,2} = \sum_{m=-\infty}^{\infty} -\left(j\omega\mu_o / (k_c)\right)\left(A_{m,2} J'_{mN} \{k_c r\} + B_{m,2} Y'_{mN} \{k_c r\} \right) \tag{13}$$

$$H_{\theta,2} = \sum_{m=-\infty}^{\infty} -\left(mN\beta / \left(k_c^2 r\right)\right)\left(A_{m,2} J_{mN} \{k_c r\} + B_{m,2} Y_{mN} \{k_c r\} \right) \tag{14}$$

where the prime indicates the differentiation of Bessel functions with respect to their argument. In equations (3) to (14), the RF dependence $\exp(j(\omega t - \beta z + mN\theta))$ is understood.

Boundary Conditions

Of the four field constants $A_{m,1}$, $B_{m,1}$, $A_{m,2}$ and $B_{m,2}$, the constant $B_{m,1}$ becomes null in order to prevent the field quantities from increasing to infinity. One may choose to express the non-zero constants $A_{m,2}$ and $B_{m,2}$ in terms of $A_{m,1}$, with the help of the following boundary conditions:

$$E_{\theta,1} = E_{\theta,2} \Big|_{r=r_V} \quad (\varphi/2 \le \theta \le 2\pi/N - \varphi/2) \tag{15}$$

$$E_{\theta,2} = 0 \Big|_{r=r_W} \quad (\varphi/2 \le \theta \le 2\pi/N - \varphi/2) \tag{16}$$

The other two boundary conditions, which are useful in the derivation of the dispersion relation of the structure, are

$$H_{\theta,1} = H_{\theta,2}\big|_{r=r_V} \qquad (\varphi/2 \le \theta \le 2\pi/N - \varphi/2) \tag{17}$$

$$H_{r,1} = 0\big|_{r=r_V} \qquad (-\varphi/2 \le \theta \le \varphi/2) \tag{18}$$

Dispersion Relation

Field matching technique is used to find the dispersion relation of the structure [1]. With the help of the boundary conditions (15-18), into which the field expressions (3-14) are substituted, we may easily find dispersion relation as,

$$\alpha_q A_{q,1} + \sum_{\substack{m=-\infty \\ m\neq q}}^{\infty} \delta_{m,q} A_{m,1} = 0 \tag{19}$$

where

$$\alpha_q = J'_{qN}\{k_C r_V\}\varphi + \left(\left(1+\eta_q\right) J_{qN}\{k_C r_V\} - \eta_q \frac{J'_{qN}\{k_C r_V\}}{Y'_{qN}\{k_C r_V\}} Y_{qN}\{k_C r_V\}\right)(2\pi/N - \varphi) \tag{20}$$

$$\delta_{m,q} = \frac{2\sin\left((m-q)(N\varphi/2)\right)}{(m-q)N} \times \left(J'_{mN}\{k_c r_V\} - \left((1+\eta_m) J_{mN}\{k_c r_V\} + \eta_m \frac{J'_{mN}\{k_c r_V\}}{Y'_{mN}\{k_c r_V\}} Y_{mN}\{k_c r_V\} \right)\right) \tag{21}$$

and

$$\eta_{m\,or\,q} = \frac{J'_{mN}\{k_c r_V\} Y'_{mN}\{k_c r_W\}}{J'_{mN}\{k_c r_W\} Y'_{mN}\{k_c r_V\} - J'_{mN}\{k_c r_V\} Y'_{mN}\{k_c r_W\}} \tag{22}$$

Considering only the three lowest-order modes of practical interest, corresponding to: a) q=0, m=1, m=-1; b) q=1, m=0, m=-1; and c) q=-1, m=0, m=1, respectively, we may write, from (19), the following set of three equations

$$\left.\begin{aligned} &\alpha_0 A_{0,1} + \delta_{1,0} A_{1,1} + \delta_{-1,0} A_{-1,1} = 0 \\ &\delta_{0,1} A_{0,1} + \alpha_1 A_{1,1} + \delta_{-1,1} A_{-1,1} = 0 \\ &\delta_{0,-1} A_{0,1} + \delta_{1,-1} A_{1,1} + \alpha_{-1} A_{-1,1} = 0 \end{aligned}\right\} \tag{23}$$

The condition for the existence of the non-trivial solutions of equation (23) is that the determinant formed by the coefficients of the constants occurring in the three simultaneous equations (23) should vanish, which simplifies to

$$\alpha_0\alpha_1\alpha_{-1} - \alpha_0\delta_{-1,1}\delta_{1,-1} + \delta_{1,0}\delta_{0,-1}\delta_{-1,1} + \delta_{1,0}\delta_{0,1}\alpha_{-1} + \delta_{-1,0}\delta_{0,1}\delta_{1,-1} - \delta_{-1,0}\delta_{0,-1}\alpha_1 = 0 \tag{24}$$

For a practical solution, the first term in the left-hand side of equation (24) dominates over the remaining terms. Therefore, retaining only the first term in the left-hand side of (24), we get

$$\alpha_0\alpha_1\alpha_{-1} = 0 \tag{25}$$

Each of the three factors of (25), equated to zero, yields the dispersion relation for each of the three possible waves. Out of these waves, the one corresponding to, $\alpha_0 = 0$, read with the help of (20), for the special case of $\phi = 0$ and $r_v = r_W$, gives $J'_0\{k_c r_W\} = 0$, the n^{th} solution of which may be identified as the dispersion relation of the TE_{0n} mode of a smooth wall cylindrical waveguide, that is, of an unloaded waveguide. In this way, the present theory of vane-loaded structure, for special case, is also validated against well-established theory of smooth wall cylindrical waveguides.

Results and Discussion

Dispersion relation (19) has been solved by using Matlab standard routine based on Powell-Dogleg method. It is of interest to study the effect of parameter variation on these characteristics. The effect of parameter variation on the characteristics of disc-loaded waveguide is shown in the Figs. (2-4). It is observed that the value of β , as well as the shape of the $\omega - \beta$ dispersion plot, depends upon the vane angular width ϕ , the number of vanes N and the vane depth r_V / r_W (the lower values of r_V / r_W corresponding to deeper vanes).

Fig. 2 reveals that cut-off frequency (lower-edge) and upper-edge frequency both increase with the decrease in the number of vanes. This upward shifting of the waveguide mode dispersion curve does not yield any appreciable enhancement of device bandwidth. But, it certainly makes the neighboring modes to be widely separated. This is highly advantageous for a particular mode selection because, in a practical device, there are almost 30 modes in only 10% band around the center frequency of the device.

Fig. 3 clearly shows that cut-off frequency of the structure decreases with the increase in the depth of vane r_V / r_W . This is because the role of the waveguide wall in defining the characteristics of the structure dominates over that of the vanes at higher values of r_V / r_W. Thus, vane depth variations does not show any fruitful bandwidth enhancement. Fig. 4 shows that the structure cut-off frequency increases with the decrease in vane angle. It shows that for a given value of ω, the value of β increases with the increase of ϕ.

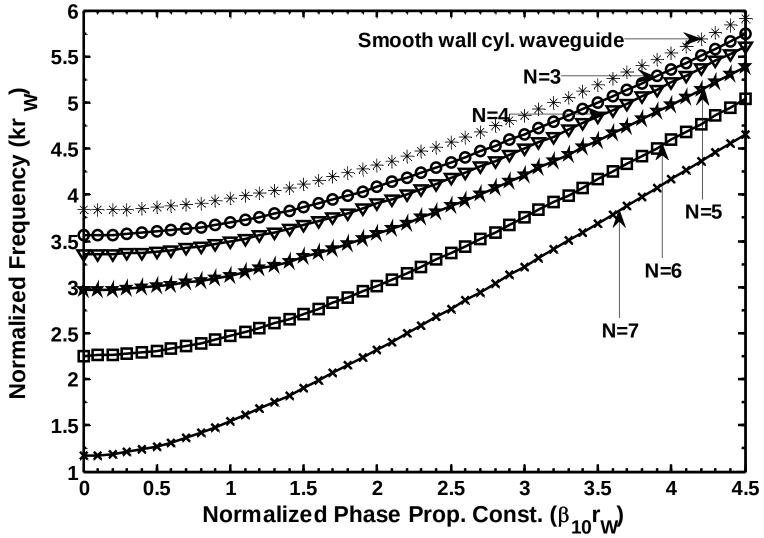

Figure 2. Dispersion characteristics of a vane-loaded circular waveguide excited in the TE_{01} mode with structure parameters $r_V / r_W = 0.8$, and ∅ = 45°; taking the number of vanes N as the parameter

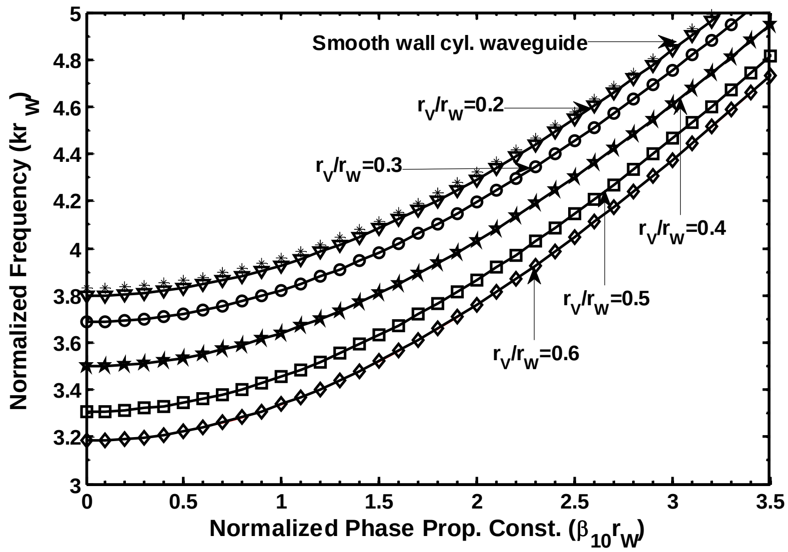

Figure 3. Dispersion characteristics of a vane-loaded circular waveguide excited in the TE_{01} mode with structure parameters N=4, and ∅ = 45°; taking the relative vane depth r_V / r_W as the parameter

It is also observed that both the shape of the $\omega - \beta$ dispersion plot and the value of β are found to be more sensitive to ϕ and N (the sensitivity increasing with the values ϕ and N) than to r_V / r_W. For the potential application of the structure in a wideband gyro-TWT, the minimum variation of the slope of the $\omega - \beta$ plot is needed to make the plot nearly linear for the desired wide-band coalescence with the beam-mode dispersion line of the device. A judicious choice of ϕ, N, and r_V / r_W can be made to achieve this.

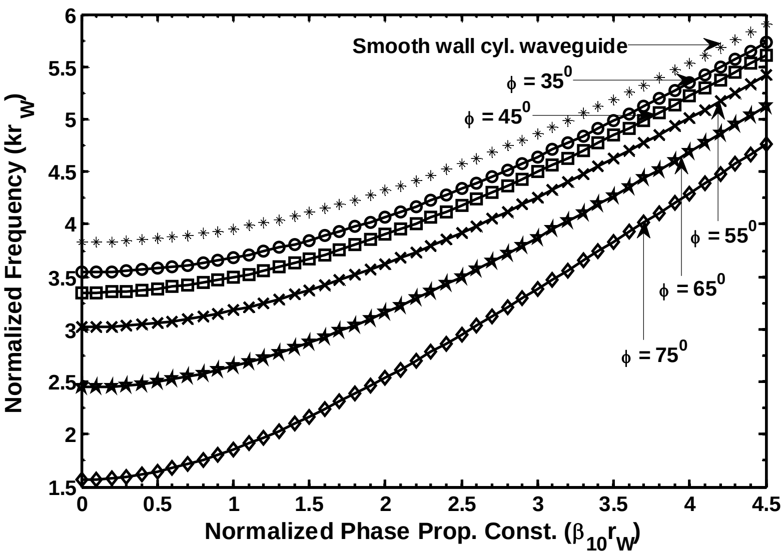

Figure 4. Dispersion characteristics of a vane-loaded circular waveguide excited in the TE_{01} mode with structure parameters N=4 and $r_V / r_W = 0.8$; taking the vane angle Øas the parameter

Fig. 5 shows the dispersion characteristics of the vane-loaded RF interaction structure and smooth wall cylindrical waveguide for azimuthally symmetric modes TE_{01}, TE_{02}, TE_{03}, and TE_{04}. It is observed that, as the mode order is increased, the cut-off frequency of the device also increases.

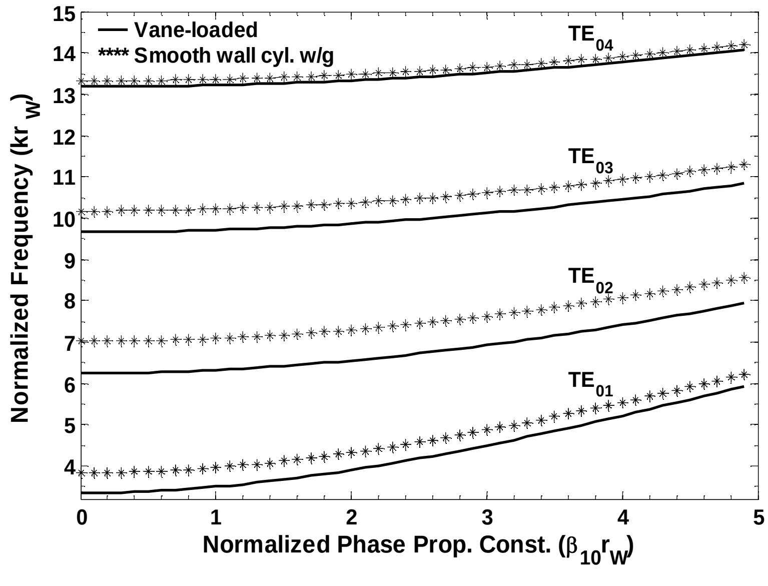

Figure 5. Dispersion characteristics of a smooth wall cylindrical waveguide and vane-loaded RF interaction structure for the azimuthally symmetric modes TE_{01}, TE_{02}, TE_{03}, and TE_{04}; taking vane structure parameters as N=4, $r_V / r_W = 0.8$, and Ø = 45^0

Conclusion

The shape of the dispersion characteristics and the value of the cutoff frequency of the vane-loaded RF interaction structure were found to depend on the vane parameters- their number as well as their radial and angular dimensions. The optimum vane parameters were obtained corresponding to the minimum variation of the slope of the $\omega - \beta$ dispersion plot, such parameters being useful from the standpoint of the bandwidth of a gyro-traveling-wave tube (gyro-TWT) using a vane-loaded cylindrical waveguide as the RF interaction structure. The dispersion characteristics were more sensitive to the number and angular width of the vanes than to their radial depth. Moreover, vane-loaded RF interaction exhibit mode rarefaction.

References

[1] B. N. Basu, Electromagnetic Theory and Applications in Beam-Wave Electronics, Singapore: World Scientific, 1996.

[2] V. L. Bratman, A. W. Gross, G. G. Denisov, W. He, A. D. R. Phelps, K. Ronald, S. V. Samsonov, C. G. Whyte, and A. R. Young, "High-Gain Wide-Band Gyrotron Travelling Wave Amplifier with a Helically Corrugated Waveguide",Phys. Rev. Lett., Vol. 84, Year 2000, Pages 2746-2749.

[3] H. S. Uhm and J. Y. Choe, "Theory of Gyrotron Amplifier in a Tape Helix Loaded Waveguide", J. Appl. Phys., Vol. 54, Year 1983, Pages 4889-4894.

[4] K. Singh, P. K. Jain, and B. N. Basu, "Analysis of Corrugated Coaxial Waveguide Resonator for Mode Rarefaction in a Gyrotron", IEEE Trans. Plasma Sci., Vol. 33, No. 3, Year 2005, Pages 1024-1030.

[5] J. Y. Choe, H. S. Uhm, and S. Ahn, "Slow Wave Gyrotron Amplifier with a Dielectric Central Rod", IEEE Trans. Microwave Theory Tech., Vol. 30, Year 1982, Pages 700-707.

[6] A. Rekiouak, B. R. Cheo, G. Wurthman, and C. Bates, "A Slow Wave Structure for Gyro-TWA H_{11}Operation", IEEE Trans. Microwave Theory Tech., Vol. 42, Year 1994, Pages 1091-1094.

[7] G. G. Denisov, V. L. Bratman, A. D. R. Phelps, and S. V. Samsonov, "Gyro-TWT with a Helical Operating Waveguide: New Possibilities to Enhance Efficiency and Frequency Bandwidth" IEEE Trans. Plasma Sci., Vol. 26, Year 1998, Pages 508-518.

[8] Y. Zhang, Y. Mo, X. Zhou, and J. Li, "Study of Disk-Loaded Waveguide Filled with Plasma",Int. J. Infrared and Millimeter Waves, Vol. 24, Year 2003, Pages 2085-2094.

[9] K. E. Kreischer, R. J. Temkin, H. R. Fetterman, and W. J. Mulligan, "Multimode Oscillation and Mode Competition in High-Frequency Gyrotrons",IEEE Trans. Microwave Theory Tech., Vol. 32, No. 5, Year 1984, Pages 481-490.